

Seasonal variability of subsurface high salinity water

A. Wang et al.

Seasonal variability of subsurface high salinity water in the northern South China Sea and its relationship with the northwestern Pacific currents

A. Wang^{1,2}, Y. Du¹, W. Zhuang¹, and Y. Qi¹

¹State Key Laboratory of Tropical Oceanography (LTO), South China Sea Institute of Oceanology, Chinese Academy of Sciences, 164 West Xingang Road, Guangzhou 510301, China

²University of Chinese Academy of Sciences, Beijing 100049, China

Received: 31 August 2014 – Accepted: 6 October 2014 – Published: 28 October 2014

Correspondence to: Y. Du (duyan@scsio.ac.cn)

Published by Copernicus Publications on behalf of the European Geosciences Union.

Title Page

Abstract

Introduction

Conclusions

References

Tables

Figures



Back

Close

Full Screen / Esc

Printer-friendly Version

Interactive Discussion



Abstract

The North Pacific Tropical Water (NPTW), characterized by the subsurface high salinity (> 34.68 PSU), is observed in the South China Sea (SCS) and often used as an indicator of the water intrusion from the northwestern Pacific into the SCS. Based on the assimilation product from a global high-resolution Hybrid Coordinate Ocean Model (HYCOM), this study investigates the seasonal variability of subsurface high salinity water (SHSW) in the northern SCS and the influence from the northwestern Pacific. Results show that there exists obvious seasonal variability in the SHSW at about 100–200 m depth. It extends as far west as 111° E in the northern SCS, reaching its volume maximum (minimum) in January (May). Further analysis shows that the seasonal change of the high salinity water is strongly affected by the seasonal variability of large-scale circulations in the low-latitude northwestern Pacific. The changes of high salinity water volume are highly correlated with the shift of the North Equatorial Current (NEC) bifurcation latitude (NECBL), which reaches the northernmost in December and the southernmost in May. Due to the large-scale wind changes in the Pacific, the Luzon Strait transport weakens (strengthens) when the NECBL shifts to the south (north) during summer (winter), which results in the reduced (enhanced) SHSW intrusion from the northwestern Pacific into the northern SCS. The velocity and salinity distribution in the Luzon Strait show that the intrusion of the SHSW mainly occurs at around 20–21.3° N.

1 Introduction

The South China Sea (SCS) is the largest marginal sea with fascinating physical processes in the northwestern Pacific. There exists subsurface high salinity water (SHSW) in the northern SCS whose variations attract much attention (e.g., Wang and Chern, 1997; Qu et al., 1999, 2000; Liu et al., 2010). The subsurface high salinity water (SHSW) is often used as the passive tracer of the North Pacific Tropical Water (NPTW) (Qu et al., 1999; Li and Wang, 2012) because of its unique water mass properties. The

OSD

11, 2423–2446, 2014

Seasonal variability of subsurface high salinity water

A. Wang et al.

Title Page

Abstract

Introduction

Conclusions

References

Tables

Figures



Back

Close

Full Screen / Esc

Printer-friendly Version

Interactive Discussion



**Seasonal variability
of subsurface high
salinity water**

A. Wang et al.

Title Page

Abstract

Introduction

Conclusions

References

Tables

Figures



Back

Close

Full Screen / Esc

Printer-friendly Version

Interactive Discussion



distribution and variation of the SHSW in the northern SCS exert significant influence on the ocean stratification and the upper circulation. The Luzon Strait (LS), located between Taiwan Island and Luzon Island, is the only deep passage connecting the SCS and the western Pacific with a maximum depth deeper than 2200 m. It is also the most influential passage that the Kuroshio affects the SCS. Previous studies indicated that the water exchange through the LS plays an important role in conveying the impact of ENSO to the SCS, modulating the SCS circulation, heat and salt budgets (Qu et al., 2004; Wang et al., 2006; Gordon et al., 2012). As one of the most important tropical Pacific current, North Equatorial Current (NEC) flows westward across the Pacific basin and bifurcates into the northward Kuroshio and southward Mindanao Current when it encounters the coast of Philippines (Nitani, 1972). As the northward-flowing Kuroshio reaches LS, it has various forms intruding into the SCS: (1) leaping across the LS to the north (Xu and Su, 1997; Su, 2001), (2) entering the SCS through a direct branch from the Kuroshio (Pu et al., 1992, 1993; Wang and Chern, 1996; Metzger and Hurlburt, 1996), (3) forming an anticyclonic loop current, which features an inflow in the southern LS and an outflow in the northern (Nitani, 1972; Farris and Wimbush, 1996; Li et al., 1996; Li and Liu, 1997), and (4) escaping into the internal SCS in the form of high frequency vortex (Wang et al., 1997; Li et al., 1998; Yuan et al., 2006). Through the water exchange in the LS, Pacific circulation can influences the SCS circulation directly.

As for seasonal variation, Wyrтки (1961) firstly mapped the winter and summer distribution of surface salinity in the SCS using in situ observations. He found that in winter there is a high salinity water tongue intruding into the SCS through the LS and extending far into the southern Vietnam along the continental shelf, while in summer the high salinity water tongue retreats. Based on the history hydrologic observations, Shaw (1991) found that the Kuroshio front meanders into the northern SCS through the LS from June to September, but does not continue to invade far west of the LS. When the northeast monsoon fully develops in late autumn to winter, water mass from the Pacific enters the SCS along the continental margin south of China and travels a distance of

Seasonal variability of subsurface high salinity water

A. Wang et al.

Title Page

Abstract

Introduction

Conclusions

References

Tables

Figures



Back

Close

Full Screen / Esc

Printer-friendly Version

Interactive Discussion



hundreds of kilometers into the SCS basin, significantly affecting the water mass characteristics in the SCS. From February to May, when the monsoon reverses its direction, the intrusion decays. Qu et al. (2000) further revealed that the Pacific subsurface high salinity water intrudes into the SCS all year-round through the LS, and has a pronounced semiannual signal with greater strength in winter and summer than in spring and autumn. From spring to autumn, the water intrusion from the Pacific is narrowly confined in the continental slope south of China. Only in winter under the influence of the full-developed northeast monsoon, the intrusion can be extended to the southern SCS. Drifting buoy observations also confirmed the obvious seasonal variability of upper Kuroshio intrusion, which is stronger in the winter (October–March) than in the summer (April–September) monsoon seasons (Centurioni et al., 2004).

However, due to the scarcity of in situ observations, the distribution and seasonal variations of the SHSW in the northern SCS are still lack of quantitative investigations. With the development of numerical simulation in recent years, the numerical model has become a powerful tool to investigate the ocean circulation and water mass changes. In the present paper, we use a state-of-the-art oceanic model assimilation product to study the SHSW distribution and the mechanisms responsible for its seasonal variability.

The rest of the paper is organized as follows. In Sect. 2 we provide a brief description of the data and method used in this study. Section 3 presents the characteristics of the high salinity water in the northern SCS and the potential forcing mechanism. A summary and discussion is given in Sect. 4.

2 Data and method

Our study is based on the Hybrid Coordinate Ocean Model (referred to as HYCOM) numerical assimilation product. Vertical coordinates in HYCOM are isopycnal in the open and stratified ocean, but smoothly transit to z coordinates in the ocean mixed layer and sigma coordinates in coastal regions. The Navy Coupled Ocean Data Assimilation

Seasonal variability of subsurface high salinity water

A. Wang et al.

Title Page

Abstract

Introduction

Conclusions

References

Tables

Figures



Back

Close

Full Screen / Esc

Printer-friendly Version

Interactive Discussion



(NCODA) system was used to assimilate satellite altimeter observation and in situ measured data from XBT and Argo. HYCOM model uses the standard Mercator coordinate with about $1/12^\circ$ horizontal resolution in tropical and subtropical area. The model has 32 vertical layers. The daily model outputs during 2008–2013 are available at <http://hycom.org> and used in this study.

The HYCOM product has been analyzed by a number of studies (e.g., Zhang and Du, 2012; Yuan et al., 2014; Zhang et al., 2010). Among others, Zhang and Du (2012) validated the reliability of HYCOM simulation based on the World Ocean Atlas (WOA) observations dataset and used the product to analyze the salinity changes in the northern Indian Ocean. Zhang et al. (2010) compared the HYCOM data with a cross-section observation in LS and found that the model well reproduces the flow pattern in the vicinity of LS. In this study, we also compare the modeled distribution of maximum salinity and its depth with the World Ocean Atlas 2001 (WOA01) observations in the northern Pacific. As shown in Fig. 1, the salinity distribution in HYCOM simulation is generally similar to WOA01. Due to the heavy spatial smooth in WOA01, the model results show more detailed and complex spatial structure. We also computed the T-S diagram (Fig. 2) using the Monthly isopycnal & Mixed-layer Ocean Climatology (MIMOC) data (Schmidtke et al., 2013). This climatology data is based mostly on Argo CTD data, supplemented by shipboard and ice-Tethered Profiler CTD data, with resolution $0.5^\circ \times 0.5^\circ$ from 80° S to 90° N. The data set is available at <http://www.pmel.noaa.gov/mimoc/>.

To provide an overview of the dynamic effects in the subsurface layer, the averaged acceleration potential ($A = p_0 \delta_0 + \int_{\delta_0}^{\delta} p d\delta$) between two layers is used. Acceleration potential is estimated by vertically integrating specific volume anomaly (p) from the reference level (Montgomery and Stroup, 1962; Reid, 1965),

$$A = p_0 \delta_0 + \int_{\delta_0}^{\delta} p d\delta \quad (1)$$

Where p is pressure, and δ_0 and p_0 are specific volume anomaly and pressure at the reference level (1500 dbar), respectively. The geostrophic velocities along isopycnals are simply determined by lateral gradients of A ,

$$(u_g, v_g) = \left(-\frac{1}{f} \frac{\partial A}{\partial y}, \frac{1}{f} \frac{\partial A}{\partial x} \right) \quad (2)$$

Where f is the Coriolis parameter.

3 Results

3.1 Spatial distribution and seasonal variation

The spatial pattern of the SHSW in the northern SCS can be well illustrated by the subsurface salinity maximum (Qu et al., 1999). Figure 1 shows that the subsurface salinity maximum water spreads westward along the NEC and extends meridionally when it encounters the Philippine coast. Some of the water migrates northward with Kuroshio and part of them further flows into the SCS across the LS. Along this spreading pathway from the NEC region to the northern SCS, the salinity maximum decreases gradually. The potential density at the salinity maximum depth increases from within the range of $23\text{--}25\sigma_\theta$ to the range of $23.5\text{--}25.5\sigma_\theta$ (Fig. 2). In this study subsurface salinity maximum in the northern SCS is restricted between 23.5 and $25.5\sigma_\theta$ layers, and we use the density range of $23.5\text{--}25.5\sigma_\theta$ to search for SHSW. Figure 3 describes the horizontal distributions of seasonal mean SHSW and their vertical depth in the study region. It is clearly seen that the maximum salinity in the western Pacific and the SCS is located among $125\text{--}150$ m. The maximum salinity is the largest in the western Pacific, and its value is larger in the northern SCS basin than in the southern SCS basin, reflecting that high salinity water in the subsurface layer of western Pacific intrudes into the SCS though the LS and then mixes with the local fresher water. Moreover, the SHSW in the northern SCS shows obvious seasonal variability. The scopes of the high salinity

Seasonal variability of subsurface high salinity water

A. Wang et al.

Title Page

Abstract

Introduction

Conclusions

References

Tables

Figures



Back

Close

Full Screen / Esc

Printer-friendly Version

Interactive Discussion



in autumn and winter are larger than those in spring and summer. In order to further investigate the seasonal variations of the SHSW in the northern SCS, we calculate the volume of the sea water salinity larger than 34.68 PSU between $23.5\sigma_\theta$ and $25.5\sigma_\theta$ within the dashed rectangle in Fig. 3. As shown in Fig. 4, the volume of the high salinity water is the largest in January and the smallest in May. The seasonal variance contribution (seasonal variance accounting for the entire variance) is 0.97. This indicates that the advection through the LS may play an important role in the intrusion of the SHSW. Since the intrusion through the LS is affected by other factors, such as the large-scale forcing of the Pacific and the strength of the Kuroshio (Yaremchuk and Qu, 2004), the relationship between the NEC and the SHSW in the northern SCS becomes an interesting question.

3.2 Impact of the tropical Northwest Pacific circulation

Upper ocean circulation in the Northwest Pacific is mainly driven by the large-scale wind. The NEC between 10–20° N band, is a stable westward current driven by wind and buoyancy flux. It splits into the poleward Kuroshio and the equatorward Mindanao Current (Nitani, 1972; Toole et al., 1990) when it encounters the coast of the Philippines, forming the so-called NEC-Mindanao Current–Kuroshio (NMK) circulation system (Qiu and Lukas, 1996). Influenced by monsoons and tropical coupled ocean–atmosphere dynamic processes, the NMK circulation system displays pronounced seasonal and interannual signals (Kim et al., 2004; Yan et al., 2014). The NEC bifurcation plays an important role in regulating the partition of mass and heat in the low-latitude west boundary (Chen, 2012; Yaremchuk and Qu, 2004). The northward-flowing Kuroshio partly intrudes into the SCS due to losing coast support when it goes by the LS, then flows southwestward along the south continental slope of China. It is obvious in Fig. 5 that the intrusion from the western Pacific into the SCS mainly occurs in autumn and winter. Especially in winter, the strong flow intrusion along the northern SCS continental slope can reach the western SCS. In summer, however, there is no significant Kuroshio intrusion and the SCS water even tends to flow back to the western

Pacific at the southeast of Taiwan. The above seasonal features are basically consistent with Qu et al. (2004). For the annual mean state, the Kuroshio in the subsurface layer is a “leaping” pattern across the LS, though there is a small loop at about 21° N (Fig. 6).

5 In order to show the vertical structure of the SHSW along the Kuroshio, we draw the seasonal mean vertical salinity profiles (Fig. 7) along the pink band in Fig. 5d. In all four seasons, the high salinity centers (greater than 34.68 PSU) exist at the depth of 100–300 m in the western Pacific, but shallow to about 80–200 m in the northern SCS. The lifting of isohalines and isopycnals occurs in the vicinity of 120° E (i.e., intrusion
10 location), probably due to the western Pacific warm water or the deep upwelling in the SCS (Nitani, 1972; Chao et al., 1996; Qu et al., 2000). During autumn-winter, the SHSW can extend westward from the Pacific to about 116° E in the SCS. In summer, by contrast, the SHSW confines to east of about 120° E, and there exists high salinity water patch in west of 120° E probably due to the activity of mesoscale eddies.

15 Figure 8 shows the seasonal-average salinity and zonal current velocity at the 120.8° E (position shown in Fig. 6). It can be seen that in all four seasons the Kuroshio intrusion through the LS is mainly confined in the upper 400 m between 20–21.3° N. While the outflow from the SCS to the western Pacific mainly occurs south of 20° N and north of 21.3° N. In the LS, salinity maximum is mainly confined between 23.5 and
20 25.5 σ_θ . Its magnitude reaches the maximum in winter and the minimum in summer.

25 Considering that the North Equatorial Current bifurcation latitude (NECBL) is an important indicator that influences the low-latitude western Pacific current system, we further discusses the correlations among the variability of the NECBL, the Kuroshio, and the SHSW in the northern SCS. In this study, the bifurcation latitude is obtained where the subsurface averaged meridional velocity is zero in the 2° band east of the Philippine coast (Qiu and Chen, 2010). Under linear wind-driven Sverdrup approximation theory, the NECBL occurs at the zero zonally integrated line of the north Pacific wind stress curl (about 14.6° N in climatological average) (Qu and Lukas, 2003). The wind-driven baroclinic Rossby wave plays a key role in the variations of the bifurcation latitude (Qiu

Seasonal variability of subsurface high salinity water

A. Wang et al.

Title Page

Abstract

Introduction

Conclusions

References

Tables

Figures



Back

Close

Full Screen / Esc

Printer-friendly Version

Interactive Discussion



and Chen, 2010). The NECBL in HYCOM simulation shows obvious annual cycle with the annual mean latitude of 14.2° N. The NECBL reaches its southernmost point (about 13.6° N) in June and northernmost (14.7° N) in December, which is basically consistent with many previous studies (e.g., Wang et al., 1997; Chen, 2012).

5 The Luzon Strait transport (LST) along 120.8° E section has distinct seasonal variations within the $23.5\text{--}25.5\sigma_{\theta}$ layers. It reaches the minimum in July and the maximum in January (Fig. 10). Using the 2004–2013 HYCOM data we find that the LST over the recent ten years decrease gradually (Figure not show). The Kuroshio transport along 18° N transect from eastern coast of the Luzon Island to 124° E (shown in Fig. 6) has
10 large seasonal variation in the subsurface layer between 23.5 and $25.5\sigma_{\theta}$. Its variation is quite different from the LST. Generally, the seasonal variation of the NECBL leads the KST three months (correlation coefficient is -0.97). When the bifurcation point shifts to north (south), the Kuroshio transport weakens (strengthens).

The seasonal time series of the LST, the NECBL, and the Kuroshio transport (KT) are shown in Fig. 10. When the NECBL shifts southward (northward), the LST decreases (increases). Previous studies considered that the change of the LST is closely related to the Kuroshio intensity east of the Luzon Island (Wang et al., 1997; Sheu et al., 2010), which was explained by Yaremchuk and Qu (2004) using the inertia effect of western boundary current. However, the result of HYCOM data shows that although
20 the seasonal variation of the NECBL is highly correlated with that of the LST (0.70), its contemporary correlation with the Kuroshio is pretty low (Fig. 10), which means that the changes of the Kuroshio intensity may be not the most important factor that controls the LST. Recent studies showed that when the westward baroclinic Rossby waves in the tropical Pacific impinge on the eastern Philippine coast, they excite coastal Kelvin waves, which propagate through the Mindoro Strait into the eastern SCS, modulate the sea level south of the Luzon Strait, and thus influence the LST (e.g., Liu et al., 2011; Zhuang et al., 2013). This dynamic process may be important for the water exchange and high salinity water intrusion through the LS.

Seasonal variability of subsurface high salinity water

A. Wang et al.

Title Page

Abstract

Introduction

Conclusions

References

Tables

Figures



Back

Close

Full Screen / Esc

Printer-friendly Version

Interactive Discussion



4 Summary and discussion

This paper analyzes the distribution and seasonal variability of the SHSW in the northern SCS based on the high-resolution HYCOM assimilation product from 2004 to 2013. The modeling results show that, during this period, the northern SCS SHSW mainly locates between 80–200 m depth and displays pronounced seasonal cycle. The volume of SHSW reaches its minimum in May and maximum in January. Further research shows that the seasonality of SHSW in the SCS is mainly influenced by the intrusion of the western Pacific NPTW through the LS at around 20–21.3° N. Part of the high salinity water flows back into the western Pacific through the 21.3–22° N of the LS. The LST and salinity flux is closely correlated with the western Pacific large scale circulation, especially the NECBL, which shifts to the northernmost in December, the southernmost in May. It indicates that the changes of western Pacific large scale circulation modulate the water exchange in the LS, and thus influence the SHSW in the interior SCS basin.

It is noteworthy that the variability of the Kuroshio transport is not exactly in phase with the NECBL and LST, probably due to the modulation of eddy activities. It means that the Kuroshio transport east of the LS is not the only factor that controls the LST. Recent studies noted another dynamic process about the impacts of Pacific on the SCS (Liu et al., 2011; Zhuang et al., 2013). When wind-driven baroclinic Rossby waves in the tropical western Pacific propagate westward and reach the eastern Philippine coast, they can excite coast Kelvin waves. The coast Kelvin waves propagate into the eastern SCS through the Sibutu Strait and Mindoro Strait, thus influence the sea level south of the LS and the transport across the strait. Due to complex dynamic processes in the northern SCS, the mechanisms of the SHSW changes are complicated. In addition to the impacts of the large scale circulations, the contribution from mesoscale eddies and local wind also needs further studies in the future.

Acknowledgements. We thank Ruixin Huang for useful advice and comments. This research was supported by the CAS/SAFEA International Partnership Program for Creative Research Teams, the Strategic Priority Research Program of Chinese Academy of Sciences (XDA11010103), the National Basic Research Program of China (2010CB950302) and the Na-

Seasonal variability of subsurface high salinity water

A. Wang et al.

Title Page

Abstract

Introduction

Conclusions

References

Tables

Figures



Back

Close

Full Screen / Esc

Printer-friendly Version

Interactive Discussion



tional Natural Science Foundation of China (Project 41176024, 41176028). We would like to acknowledge the National Ocean Partnership Program (NOPP) for providing the high resolution HYCOM data (<http://hycom.org/dataserver/>). The MIMOC product was provided by the NASA (<http://www.pmel.noaa.gov/mimoc/>). The WOA01 was obtained from the Ocean Climate Laboratory, NODC (<http://www.nodc.noaa.gov/OC5/WOA01/woa01dat.html>).

References

- Chao, S.-Y., Shaw, P. T., and Wu, S. Y.: Deep sea ventilation in the South China Sea, *Deep-Sea Res. Pt. I*, 43, 445–466, 1996.
- Chen, Z. H.: Study on the multi time scale variability and dynamics of the North Equatorial Current Bifurcation in the Pacific, Ph.D. thesis, Ocean University of China, Qingdao, 114 pp., 2012 (in Chinese).
- Centurioni, L. R., Niiter, P. P., and Lee, D. K.: Observations of inflow of Philippine Sea surface water into the South China Sea through the Luzon Strait, *J. Phys. Oceanogr.*, 34, 113–121, 2004.
- Farris, A. and Wimbush, M.: Wind-induced Kuroshio intrusion into the South China Sea, *J. Oceanogr.*, 52, 771–784, 1996.
- Gordon, A. L., Huber, B. A., Metzger, E. J., Susanto, R. D., Hurlburt, H. E., and Adi, T. R.: South China Sea throughflow impact on the Indonesian throughflow, *Geophys. Res. Lett.*, 39, L11602, 2012.
- Kim, Y. Y., Qu, T., Jensen, T., Miyama, T., Mitsudera, H., Kang, H.-W., and Ishida, A.: Seasonal and interannual variations of the North Equatorial Current bifurcation in a high-resolution OGCM, *J. Geophys. Res.*, 109, C03040, doi:10.1029/2003JC002013, 2004.
- Li, L., Nowlin, W. D., and Su, J. L.: Anticyclonic rings from the Kuroshio in the South China Sea, *Deep-Sea Res. Pt. I*, 45, 1469–1482, 1998.
- Li, W. and Liu, Q. Y.: A preliminary study of the deformation and its dynamics of western boundary current at a gap, *Journal of Ocean University of Qingdao*, 27, 277–281, 1997 (in Chinese).
- Li, W., Liu, Q. Y., and Cheng, S.-P.: The effect of break in western boundary on the western boundary current, *Acta Oceanographica Taiwanica*, 35, 141–153, 1996.

Seasonal variability of subsurface high salinity water

A. Wang et al.

Title Page

Abstract

Introduction

Conclusions

References

Tables

Figures



Back

Close

Full Screen / Esc

Printer-friendly Version

Interactive Discussion



Seasonal variability of subsurface high salinity water

A. Wang et al.

Title Page

Abstract

Introduction

Conclusions

References

Tables

Figures



Back

Close

Full Screen / Esc

Printer-friendly Version

Interactive Discussion



- Li, Y. L. and Wang, F.: Spreading and salinity change of North Pacific Tropical Water in the Philippine Sea, *J. Oceanogr.*, 68, 439–452, 2012.
- Liu, Q. Y., Feng, M., and Wang, D. X.: ENSO-induced interannual variability in the southeastern South China Sea, *J. Oceanogr.*, 67, 127–133, 2011.
- 5 Liu, Y., Bye, J. A., You, Y., Bao, X., and Wu, D.: The flushing and exchange of the South China Sea derived from salt and mass conservation, *Deep-Sea Res. Pt. II*, 57, 1212–1220, 2010.
- Metzger, E. J. and Hurlburt, H. E.: Coupled dynamics of the South China sea, the Sulu sea, and the Pacific ocean, *J. Geophys. Res.-Oceans*, 101, 12331–12352, 1996.
- 10 Montgomery, R. B. and Stroup, E. D.: Equatorial Waters and Currents at 150° W in July–August 1952: Tome 1, 1962.
- Nitani, H.: Beginning of the Kuroshio, in: *Kuroshio: Its Physical Aspects*, edited by: Stommel, H. and Yoshida, K., University of Tokyo Press, Tokyo, 129–163, 1972.
- Pu, S. Z., Yu, H. L., and Jiang, S. N.: Branchings of Kuroshio into Bashi Channel and South China Sea, *Tropic Oceanology*, 11, 1–8, 1992 (in Chinese).
- 15 Pu, S. Z., Yu, H. L., and Jiang, S. N.: The upper layer circulation in the Bashi Channel and the northeastern South China Sea, in: *Proceedings of the Symposium on the Physical and Chemical Oceanography of the China Seas*, China Ocean Press, Beijing, 10–18, 1993.
- Qiu, B. and Chen, S.: Interannual-to-decadal variability in the bifurcation of the north equatorial current off the Philippines, *J. Phys. Oceanogr.*, 40, 2525–2538, 2010.
- 20 Qiu, B. and Lukas, R.: Seasonal and interannual variability of the North Equatorial Current, the Mindanao Current, and the Kuroshio along the Pacific western boundary, *J. Geophys. Res.*, 101, 12315–12330, 1996.
- Qu, T. and Lukas, R.: The bifurcation of the north equatorial current in the Pacific, *J. Phys. Oceanogr.*, 33, 5–18, 2003.
- 25 Qu, T., Mitsudera, H., and Yamagata, T.: A climatology of the circulation and water mass distribution near the Philippine coast*, *J. Phys. Oceanogr.*, 29, 1488–1505, 1999.
- Qu, T., Mitsudera, H., and Yamagata, T.: Intrusion of the North Pacific waters into the South China Sea, *J. Geophys. Res.-Oceans*, 105, 6415–6424, 2000.
- 30 Qu, T., Kim, Y. Y., Yaremchuk, M., Tozuka, T., Ishida, A., and Yamagata, T.: Can Luzon strait transport play a role in conveying the impact of ENSO to the South China Sea?, *J. Climate*, 17, 3644–3657, 2004.
- Reid Jr., J. L.: *Intermediate waters of the Pacific Ocean* (No. JHU), Scripps Institution of Oceanography, La Jolla, CA, 1965.

Seasonal variability of subsurface high salinity water

A. Wang et al.

Title Page

Abstract

Introduction

Conclusions

References

Tables

Figures



Back

Close

Full Screen / Esc

Printer-friendly Version

Interactive Discussion



- Shaw, P. T.: The seasonal variation of the intrusion of the Philippine Sea water into the South China Sea, *J. Geophys. Res.-Oceans*, 96, 821–827, 1991.
- Shaw, P. T. and Chao, S. Y.: Surface circulation in the South China Sea, *Deep-Sea Res. Pt. I*, 41, 1663–1683, 1994.
- 5 Sheu, W. J., Wu, C. R., and Oey, L. Y.: Blocking and westward passage of eddies in the Luzon Strait, *Deep-Sea Res. Pt. II*, 57, 1783–1791, 2010.
- Schmidtko, S., Johnson, G. C., and Lyman, J. M.: MIMOC: a global monthly isopycnal upper-ocean climatology with mixed layers, *J. Geophys. Res.*, 118, 1658–1672, doi:10.1002/jgrc.20122, 2013.
- 10 Su, J. L.: A review of circulation dynamics of the coastal oceans near China, *Acta Oceanol. Sin.*, 23, 1–16, 2001.
- Tian, J., Yang, Q., Liang, X., Xie, L., Hu, D., Wang, F., and Qu, T.: Observation of Luzon Strait transport, *Geophys. Res. Lett.*, 33, L19607, doi:10.1029/2006GL026272, 2006.
- Toole, J. M., Millard, R. C., Wang, Z., and Pu, S.: Observations of the Pacific North Equatorial Current bifurcation at the Philippine coast, *J. Phys. Oceanogr.*, 20, 307–318, 1990.
- 15 Wang, D., Liu, Q., Huang, R. X., Du, Y., and Qu, T.: Interannual variability of the South China Sea throughflow inferred from wind data and an ocean data assimilation product, *Geophys. Res. Lett.*, 33, L14605, doi:10.1029/2006GL026316, 2006.
- Wang, J. and Chern, C. S.: Some aspects on the circulation in the northern South China Sea, *La Mer*, 34, 246–257, 1996.
- 20 Wang, J. and Chern, C. S.: On the trajectory of subsurface and intermediate waters in the north-eastern South China Sea, *Journal of Tropical Oceanography*, 16, 24–41, 1997 (in Chinese).
- Wyrski, K.: *Physical Oceanography of the Southeast Asian Waters*, The University of California Scripps Institution of Oceanography, La Jolla, CA, 1961.
- 25 Xu, J. P. and Su, J. L.: Hydrographic analysis on the intrusion of the Kuroshio into the South China Sea II. Observational results during the cruise from August to September in 1994, *Journal of Tropical Oceanography*, 16, 1–23, 1997 (in Chinese).
- Yan, Q., Hu, D., and Zhai, F.: Seasonal variability of the North Equatorial Current transport in the western Pacific Ocean, *Chinese journal of oceanology and limnology*, 32, 223–237, 2014.
- 30 Yaremchuk, M. and Qu, T.: Seasonal variability of the large-scale currents near the coast of the Philippines coast, *J. Phys. Oceanogr.*, 34, 844–855, 2004.
- Yuan, D., Han, W., and Hu, D.: Surface Kuroshio path in the Luzon Strait area derived from satellite remote sensing data, *J. Geophys. Res.-Oceans*, 111, 2006.

Yuan, Y., Tseng, Y. H., Yang, C., Liao, G., Chow, C. H., Liu, Z., Zhu, X., and Chen, H.: Variation in the Kuroshio intrusion: modeling and interpretation of observations collected around the Luzon Strait from July 2009 to March 2011, *J. Geophys. Res.*, 119, 3447–3463, 2014.

5 Zhang, Y. H. and Du, Y.: Seasonal variability of salinity budget and water exchange in the northern Indian Ocean from HYCOM assimilation, *Chin. J. Oceanol. Limn.*, 30, 1082–1092, 2012.

Zhang, Z., Zhao, W., and Liu, Q.: Sub-seasonal variability of Luzon strait transport in a high resolution global model, *Acta Oceanol. Sin.*, 29, 9–17, 2010.

10 Zhuang, W., Qiu, B., and Du, Y.: Low-frequency Western Pacific Ocean sea level and circulation changes due to the connectivity of the Philippine archipelago, *J. Geophys. Res.-Oceans*, 118, 6759–6773, 2013.

Seasonal variability of subsurface high salinity water

A. Wang et al.

Title Page

Abstract

Introduction

Conclusions

References

Tables

Figures



Back

Close

Full Screen / Esc

Printer-friendly Version

Interactive Discussion



Seasonal variability of subsurface high salinity water

A. Wang et al.

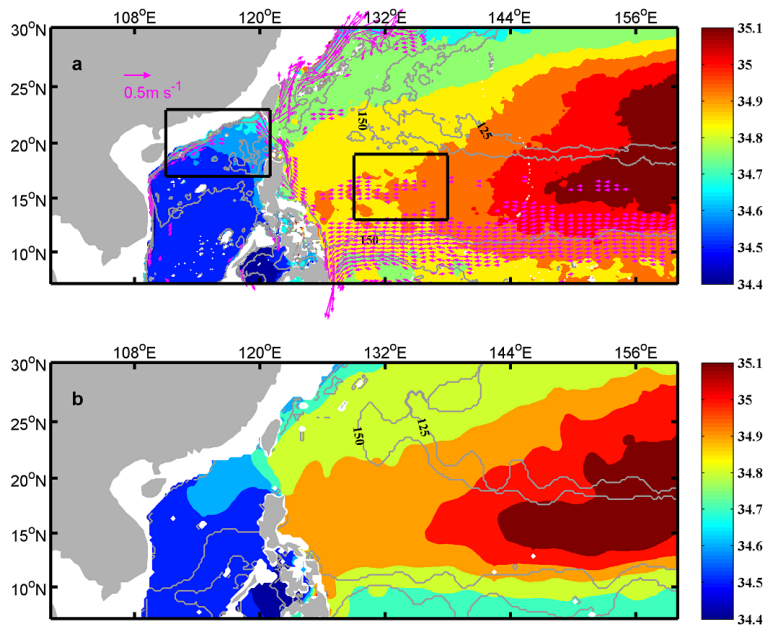


Figure 1. Distribution of the maximum salinity (color shading; PSU) and its depth (grey contours; m): **(a)** HYCOM; **(b)** WOA01. The boxes show the regions used for T-S analysis in Fig. 2. Subsurface currents (vectors, pink) larger than 0.1 m s^{-1} are superimposed.

Title Page

Abstract

Introduction

Conclusions

References

Tables

Figures



Back

Close

Full Screen / Esc

Printer-friendly Version

Interactive Discussion



Seasonal variability of subsurface high salinity water

A. Wang et al.

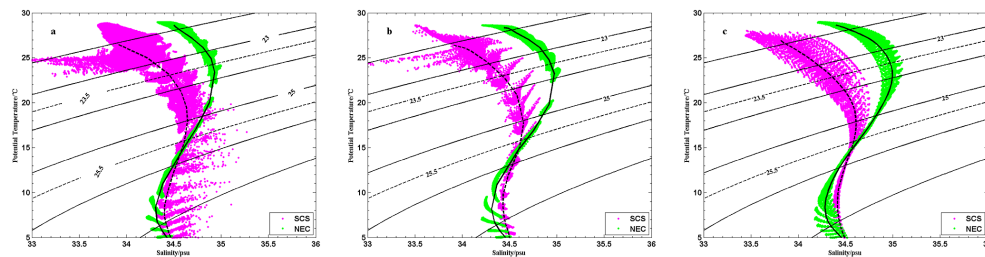


Figure 2. T-S diagram at the two black boxes in Fig. 1: **(a)** HYCOM; **(b)** WOA01; **(c)** MIMOC. Pink and green dots represent the selected waters in the SCS and NEC, respectively.

[Title Page](#)[Abstract](#)[Introduction](#)[Conclusions](#)[References](#)[Tables](#)[Figures](#)[Back](#)[Close](#)[Full Screen / Esc](#)[Printer-friendly Version](#)[Interactive Discussion](#)

Seasonal variability of subsurface high salinity water

A. Wang et al.

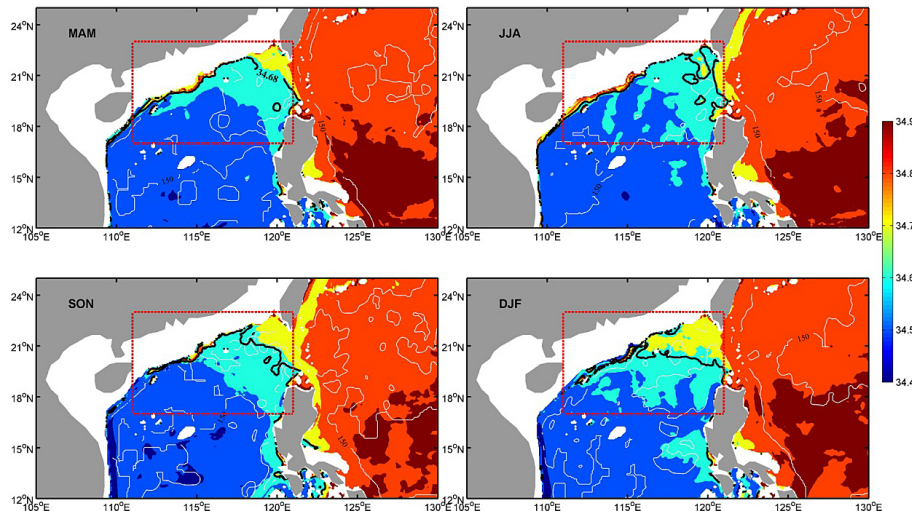


Figure 3. The salinity maximum (shaded; PSU) and depth (grey contours; m) between 23.5 and 25.5 σ_θ in the SCS. Black contours represent 34.68 PSU and red dotted box is our computation domain.

[Title Page](#)[Abstract](#)[Introduction](#)[Conclusions](#)[References](#)[Tables](#)[Figures](#)[◀](#)[▶](#)[◀](#)[▶](#)[Back](#)[Close](#)[Full Screen / Esc](#)[Printer-friendly Version](#)[Interactive Discussion](#)

Seasonal variability of subsurface high salinity water

A. Wang et al.

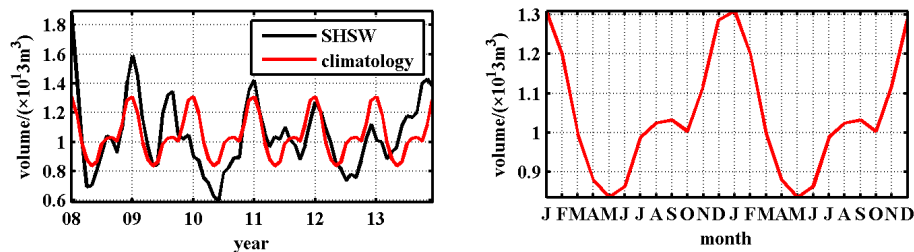


Figure 4. Variation of the subsurface high salinity water (SHSW) in the northern SCS. SHSW is defined the water salinity higher than 34.68 PSU in 111–121° E, 17–23° N between 23.5 and $25.5\sigma_\theta$. 3 month running mean filter has been applied to remove high frequency variations.

[Title Page](#)[Abstract](#)[Introduction](#)[Conclusions](#)[References](#)[Tables](#)[Figures](#)[Back](#)[Close](#)[Full Screen / Esc](#)[Printer-friendly Version](#)[Interactive Discussion](#)

Seasonal variability of subsurface high salinity water

A. Wang et al.

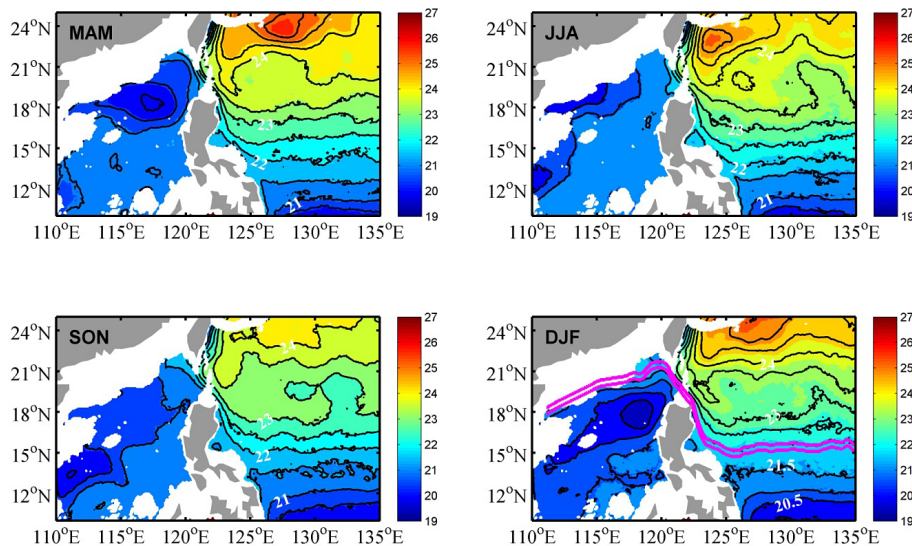


Figure 5. Seasonally acceleration potential ($\text{m}^2 \text{s}^{-2}$) averaged between 23.5 and $25.5\sigma_\theta$.

Title Page

Abstract

Introduction

Conclusions

References

Tables

Figures

◀

▶

◀

▶

Back

Close

Full Screen / Esc

Printer-friendly Version

Interactive Discussion



Seasonal variability of subsurface high salinity water

A. Wang et al.

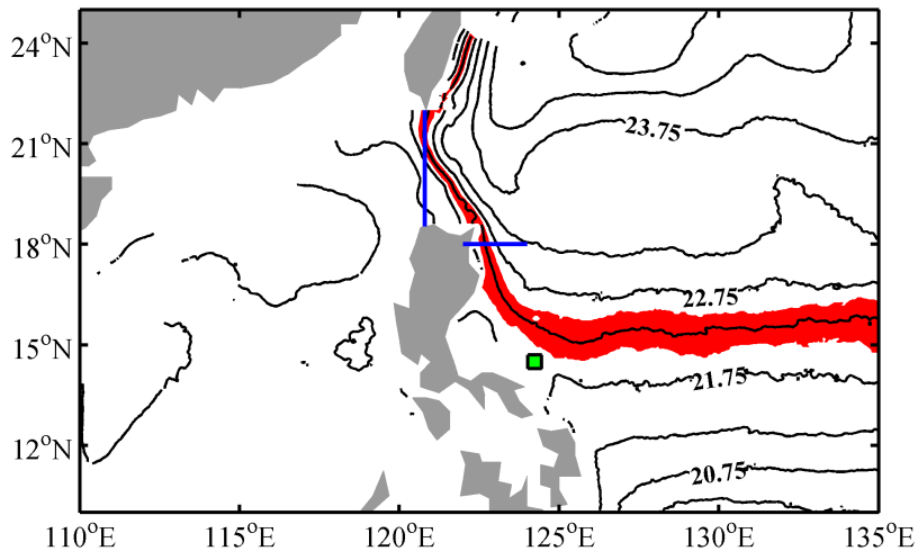


Figure 6. Same as Fig. 5 except for annual average (contours). The red stripe represents the pathway of the NK. Green box indicates the location of the mean NEC bifurcation. The two blue lines indicate the location for computing KT and LST, respectively.

[Title Page](#)[Abstract](#)[Introduction](#)[Conclusions](#)[References](#)[Tables](#)[Figures](#)[◀](#)[▶](#)[◀](#)[▶](#)[Back](#)[Close](#)[Full Screen / Esc](#)[Printer-friendly Version](#)[Interactive Discussion](#)

Seasonal variability of subsurface high salinity water

A. Wang et al.

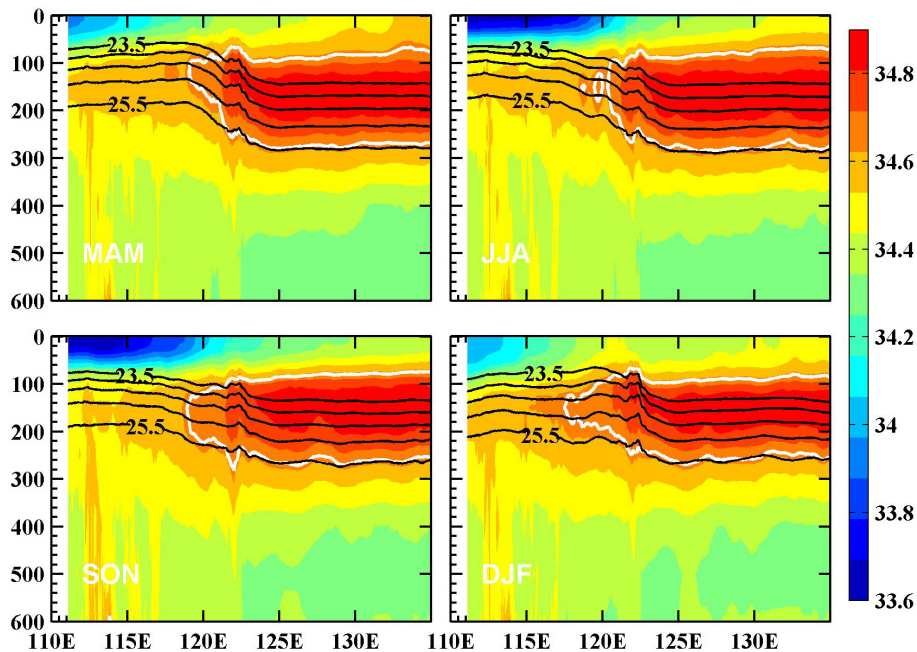


Figure 7. Salinity (shaded; PSU) and potential density (black contours; kg m^{-3}) along the flow in pink color in Fig. 5. The white contours represent the 34.68 PSU salinity.

Title Page

Abstract

Introduction

Conclusions

References

Tables

Figures

◀

▶

◀

▶

Back

Close

Full Screen / Esc

Printer-friendly Version

Interactive Discussion



Seasonal variability of subsurface high salinity water

A. Wang et al.

Title Page

Abstract

Introduction

Conclusions

References

Tables

Figures

◀

▶

◀

▶

Back

Close

Full Screen / Esc

Printer-friendly Version

Interactive Discussion

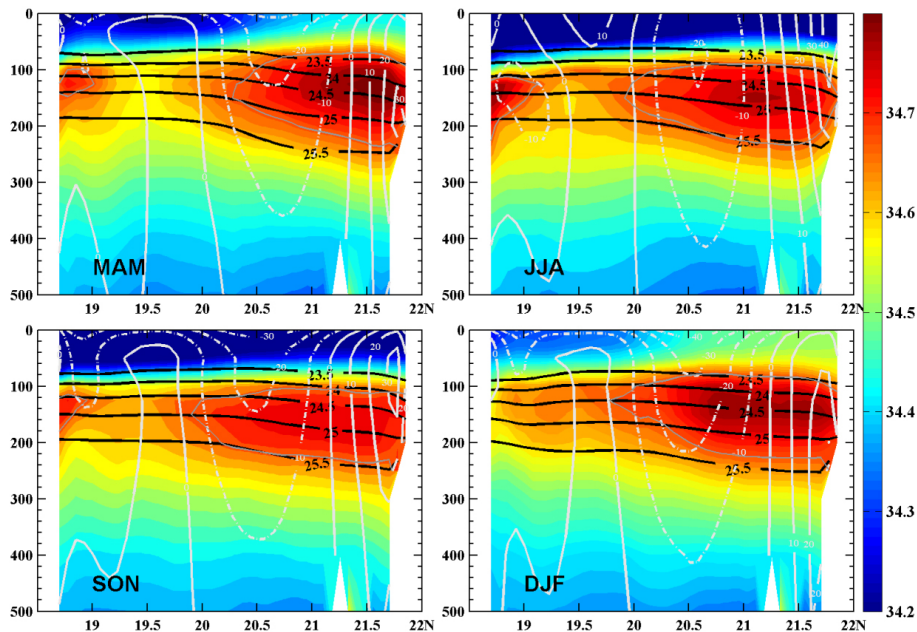


Figure 8. Seasonal salinity (shaded; PSU) and zonal velocity (white contours; cm s^{-1}) along the Luzon Strait (120.8°E). Black lines represent the potential density. Grey contours indicate 34.68 PSU salinity. Positive (negative) values represent eastward (westward) currents.

Seasonal variability of subsurface high salinity water

A. Wang et al.

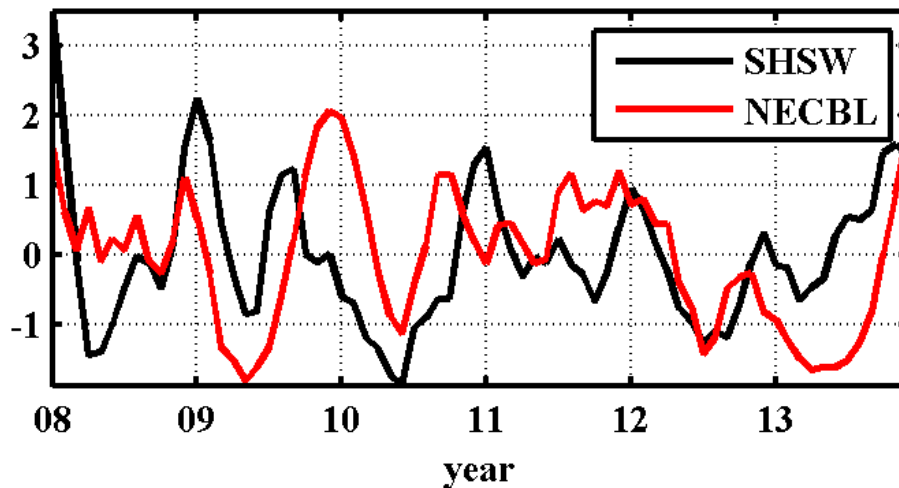


Figure 9. Seasonal variation of the subsurface high salinity water (SHSW) in the northern SCS and the NEC bifurcation latitude (NECBL) (all normalized after applying 3-month smoothing average). Correlation coefficient between them is 0.27 (98 % confidence).

[Title Page](#)[Abstract](#)[Introduction](#)[Conclusions](#)[References](#)[Tables](#)[Figures](#)[◀](#)[▶](#)[◀](#)[▶](#)[Back](#)[Close](#)[Full Screen / Esc](#)[Printer-friendly Version](#)[Interactive Discussion](#)

Seasonal variability of subsurface high salinity water

A. Wang et al.

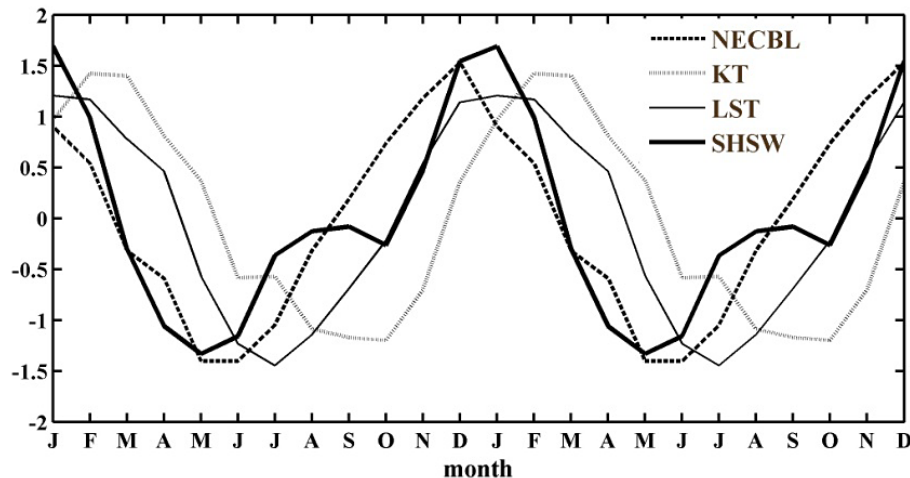


Figure 10. Seasonal variation of the NEC bifurcation latitude (NECBL), the Kuroshio transport (KT), the Luzon Strait transport (LST), and the subsurface high salinity water (SHSW) in the northern SCS (all normalized after applying 3 month running mean filter).

Title Page

Abstract

Introduction

Conclusions

References

Tables

Figures

◀

▶

◀

▶

Back

Close

Full Screen / Esc

Printer-friendly Version

Interactive Discussion

